Possibilities for Improved Early Breast Cancer Detection by Padé-Optimized Magnetic Resonance Spectroscopy

Karen Belkić MD PhD[1,2,3] and Dževad Belkić PhD[1]

[1]Department of Oncology/Pathology, Karolinska Institute, Stockholm, Sweden
[2]Claremont Graduate University, School of Community and Global Health, Claremont, CA, USA
[3]Institute for Prevention Research, University of Southern California School of Medicine. Los Angeles, CA, USA

ABSTRACT: There are major dilemmas regarding the optimal modalities for breast cancer screening. This is of particular relevance to Israel because of its high-risk population. It was suggested that an avenue for further research would be to incorporate advances in signal processing through the fast Padé transform (FPT) to magnetic resonance spectroscopy (MRS). We have now applied the FPT to time signals that were generated according to in vitro MRS data as encoded from extracted breast specimens from normal, non-infiltrated breast tissue, fibroadenoma and cancerous breast tissue. The FPT is shown to resolve and precisely quantify the physical resonances as encountered in normal versus benign versus malignant breast. The FPT unambiguously delineated and quantified diagnostically important metabolites such as lactate, as well as phosphocholine, which very closely overlaps with glycerophosphocholine and phosphoethanolamine, and may represent a magnetic resonance-visible molecular marker of breast cancer. These advantages of the FPT could clearly be of benefit for breast cancer diagnostics via MRS. This line of investigation should continue with encoded data from benign and malignant breast tissue, in vitro and in vivo. We anticipate that Padé-optimized MRS will reduce the false positive rates of MR-based modalities and further improve their sensitivity. Once this is achieved, and given that MR entails no exposure to ionizing radiation, new possibilities for screening and early detection emerge, especially for risk groups. For example, Padé-optimized MRS together with MR imaging could be used with greater surveillance frequency among younger women with high risk of breast cancer.

IMAJ 2011; 13: 236–243

KEY WORDS: magnetic resonance spectroscopy, breast cancer, early detection, signal processing, high risk

The Jewish population of Israel born in Europe or North America has among the highest age-standardized incidence rates of breast cancer in the world [1]. Ashkenazi Jewish ethnicity is included as a risk factor for breast cancer both by the U.S. National Comprehensive Cancer Network [2] and the National Breast Cancer Centre of Australia [3]. One contributory factor is the estimated 2.5% likelihood of carrying a deleterious *BRCA*1/2 mutation among the Ashkenazi Jewish population, compared for example to the general western European population for whom the probability is approximately 0.2% [4,5]. Lifestyle factors and exposures may also contribute [6-10]. It was recently reported that Israeli women who were likely to have been directly exposed to the Holocaust were at significantly increased breast cancer risk compared to age-matched Israeli women of European origin without direct exposure to the Holocaust [10].

Israel has a national screening program aimed at early detection of breast cancer. The need to continue and even expand this program has been emphasized in light of the high risk of many in the population [11], as well as the need for special outreach to groups with low participation [12]. Today, however, some controversy exists regarding the optimal modalities for breast cancer screening, especially when applied to women at risk [13]. Systematic early detection through screening with mammography followed by appropriate diagnosis and management have been demonstrated to significantly reduce mortality from breast cancer [4,14]. Mammography has been the mainstay of breast cancer screening but has relatively poor specificity. For dense breasts, seen particularly in young women, its sensitivity is also low.

Magnetic resonance-based modalities can aid in early breast cancer detection without exposing the breast, a radiosensitive tissue, to ionizing radiation. This is of particular concern in view of the heightened radiosensitivity in women with genetic risk for breast cancer, and because screening for women at high risk should begin at a younger age and with increased frequency [15,16]. Contrast-enhanced magnetic resonance imaging is usually very sensitive, particularly in women with an increased breast cancer risk [4]. While false negative findings have been reported for MRI on rare occasions, the main problem with MRI is that its specificity is poorer than that of mammography [4,17]. This results in higher callback and biopsy rates, with fewer than 50% of these biopsies showing

FPT = fast Padé transform
MRS = magnetic resonance spectroscopy

cancer [4]. Benign lesions such as fibroadenomas are sometimes difficult to distinguish from breast cancer on MRI [18]. Consequently, while women at high risk for breast cancer participating in intensive surveillance programs appear to be relieved due to the greater sensitivity of MRI [19], the large number of false positive findings may adversely affect quality of life [13,20].

Magnetic resonance-based diagnostics entail no exposure to ionizing radiation and have a high sensitivity in breast cancer detection

Magnetic resonance spectroscopy provides insight into the metabolic characteristics of tissue, and improves the specificity of MRI vis-à-vis breast cancer diagnostics [21,22]. An analysis of over 100 malignant and 100 benign breast lesions was recently published [23]. These studies were mainly based on the composite choline signal. However, relying on the composite choline peak can undermine diagnostic accuracy, since choline may also be detected in fibroadenomas and other benign breast lesions as well as during lactation and may be undetected in small tumors that are then misclassified as benign [21].

To date, MRS has relied almost exclusively on the conventional theoretical framework for data analysis in biomedical imaging, namely, the fast Fourier transform, which is a mathematical procedure for converting the encoded time signal into its spectral representation in the frequency domain. Several intrinsic limitations of the FFT are specifically relevant to breast cancer diagnostics using MRS, including poor resolution and signal-to-noise ratio and having to rely on estimates of a single composite compound (total choline) [13,23,24]. In vitro NMR (nuclear magnetic resonance) applied to extracted specimens can provide greater insight into the metabolic activity of cancerous breast tissue. We have performed multivariate analyses [13] of such NMR data from extracted breast specimens [25], which yielded rich spectroscopic information for detecting breast cancer in closely overlapping resonances. Several metabolites improved diagnostic accuracy (notably lactate), while total choline had somewhat lower diagnostic accuracy compared to its closely overlapping components and a number of other metabolites. Further exploration of how MRS could tap into this rich store of metabolic information was therefore recommended, using improved signal processing methods to quantify MR-visible compounds in breast lesions [13].

The fast Padé transform has been suggested as the optimal signal processing method for MRS [13,23,26-28]. The FPT is a high-resolution non-linear parametric signal processor, defined by the ratio of two polynomials. The FPT determines the exact number of metabolites and the spectral parameters from which metabolite concentrations, including those from very closely overlapping resonances, can be unequivocally computed [13,23, 26-28]. We recently examined the performance of the FPT applied to time signals that were generated according to in vitro MRS data as encoded from extracted breast specimens [25]. The in-depth mathematical background and numerical results have been published [23,24]. In the present review we emphasize the clinical implications, focusing on how the Padé-optimized MRS could potentially be used to improve early breast cancer detection.

Advances in signal processing via the fast Padé transform can resolve magnetic resonance-visible markers of breast cancer

METHODS

The FPT was applied to time signals similar to in vitro MRS data as encoded from extracted breast specimens [25]. Three time signals corresponding to normal, non-infiltrated breast, fibroadenoma and breast cancer were generated. These time signals $\{c_n\}$ were sampled from the sums of complex damped harmonics, $c_n = \sum_{k=1}^{K} d_k e^{in\tau\omega_k} (0 \le n \le N - 1)$ where N is the total signal length. Here, the d_k's are the stationary amplitudes and τ is the sampling time ($\tau = T/N$). Further, the ω_k's are the complex fundamental frequencies with $\mathrm{Im}(\omega_k) > 0 \ (1 \le k \le K)$, where K is the total number of harmonics, which is set to $K = 9$, according to Gribbestad et al. [25]. The time signals were then quantified using the FPT, as per a previous study [28]. The input peak amplitudes $\{|d_k|\}$ were computed from the reported concentrations $\{C_k\}$ via $|d_k| = 2C_k/C_{ref}$, where $C_{ref} = 0.05$ μM/g ww, and ww signifies wet weight. Also, TSP (3-(trimethylsilyl-3,3,2,2-tetradeutero-propionic acid) was used as the internal reference from Gribbestad's study [25], such that $|d_k| = C_k / (25\mu\mathrm{M/g\ ww})$. We used the median concentrations expressed in μM/g ww of nine metabolites from the data of that study [25] based upon tissue samples from twelve patients for normal non-infiltrated breast to compute the input amplitudes $|d_k|$. For the fibroadenoma, the concentrations of the nine metabolites were based on data from a single patient [25]. The median concentrations for seven of the metabolites for breast cancer were from fourteen samples taken from twelve patients (in two patients, two malignant samples were taken) [25]. The median concentrations of the other metabolites, β-glucose and myoinositol, were based upon six and nine malignant samples, respectively.

A static magnetic field of $B_0 \approx 14.1$T (Larmor frequency of 600 MHz) was used in the recording of the time signals from that study [25]. We used a bandwidth of 6 kHz (the inverse of this bandwidth is the sampling time τ) and set the total signal length $N = 2048$. The full widths at half maximum were taken to be approximately 1 Hz, with small variations [23,24]. The peaks were assumed to be Lorentzian. The phases ϕ_k $(1 \le k \le 9)$ from complex-valued d_k were all

FFT = fast Fourier transform
NMR = nuclear magnetic resonance

Table 1. Input data for normal breast, fibroadenoma and breast cancer derived from Ref. [25] (left columns) and Padé-reconstructed peak positions, heights and metabolite concentrations at partial signal length N_P =1000 (prior to convergence-middle columns) and at N_P =1500 (full convergence – right columns)

		Input data			Padé-reconstructed N_P= 1000			Padé-reconstructed N_P= 1500		
		Position	Height	Concentration	Position	Height	Concentration	Position	Height	Concentration
Normal breast (i)	1. Lac	1.3304	0.0202	0.504	1.3304	0.0202	0.504	1.3304	0.0202	0.504
	2. Ala	1.4703	0.0035	0.088	1.4703	0.0035	0.088	1.4703	0.0035	0.088
	3. Cho	3.2101	0.0007	0.017	3.2101	0.0007	0.017	3.2101	0.0007	0.017
	4. PCho	3.2200	0.0008	0.019	--	--	--	3.2200	0.0008	0.019
	5. PE	3.2202	0.0052	0.129	3.2202	0.0059	0.148	3.2202	0.0052	0.129
	6. GPC	3.2304	0.0013	0.032	3.2304	0.0013	0.032	3.2304	0.0013	0.032
	7. β-Glc	3.2502	0.0180	0.450	3.2502	0.0180	0.450	3.2502	0.0180	0.450
	8. Tau	3.2701	0.0053	0.133	3.2701	0.0053	0.133	3.2701	0.0053	0.133
	9. m-Ino	3.2801	0.0114	0.286	3.2801	0.0114	0.286	3.2801	0.0114	0.286
Fibro-adenoma (ii)	1. Lac	1.3304	0.0593	1.482	1.3304	0.0593	1.482	1.3304	0.0593	1.482
	2. Ala	1.4703	0.0044	0.110	1.4703	0.0044	0.110	1.4703	0.0044	0.110
	3. Cho	3.2101	0.0009	0.022	3.2101	0.0009	0.022	3.2101	0.0009	0.022
	4. PCho	3.2200	0.0043	0.108	--	--	--	3.2200	0.0043	0.108
	5. PE	3.2202	0.0148	0.369	3.2202	0.0191	0.477	3.2202	0.0148	0.369
	6. GPC	3.2304	0.0028	0.069	3.2304	0.0028	0.069	3.2304	0.0028	0.069
	7. β-Glc	3.2502	0.0391	0.978	3.2502	0.0391	0.978	3.2502	0.0391	0.978
	8. Tau	3.2701	0.0135	0.338	3.2701	0.0135	0.338	3.2701	0.0135	0.338
	9. m-Ino	3.2801	0.0186	0.465	3.2801	0.0186	0.465	3.2801	0.0186	0.465
Breast cancer (iii)	1. Lac	1.3304	0.3247	8.119	1.3304	0.3247	8.119	1.3304	0.3247	8.119
	2. Ala	1.4703	0.0316	0.789	1.4703	0.0316	0.789	1.4703	0.0316	0.789
	3. Cho	3.2101	0.0045	0.112	3.2101	0.0044	0.111	3.2101	0.0045	0.112
	4. PCho	3.2200	0.0245	0.612	--	--	--	3.2200	0.0245	0.612
	5. PE	3.2202	0.0778	1.944	3.2202	0.1023	2.558	3.2202	0.0778	1.944
	6. GPC	3.2304	0.0094	0.234	3.2304	0.0093	0.233	3.2304	0.0094	0.234
	7. β-Glc	3.2502	0.0288	0.721	3.2502	0.0288	0.720	3.2502	0.0288	0.721
	8. Tau	3.2701	0.1118	2.796	3.2701	0.1118	2.795	3.2701	0.1118	2.796
	9. m-Ino	3.2801	0.0356	0.891	3.2801	0.0356	0.891	3.2801	0.0356	0.891

Hereafter, positions are in parts per million (ppm), heights in arbitrary units (au), concentrations in μM/g ww

Lac = lactate, Ala = alanine, Cho =choline, PCho = phosphocholine, PE = phosphoethanolamine, GPC = glycerophosphocholine, β-Glc = β-glucose, Tau = taurine, m-Ino =myoinositol.

set to zero, such that each d_k becomes real, $d_k = |d_k|$.

The left panel of Table 1 displays the input positions, peak heights and concentrations for normal breast [top rows, (i)], fibroadenoma [middle rows (ii)] and breast cancer [lower rows (iii)]. The FPT extracts K and the parameters $\{\omega_k, d_k\}(1 \le k \le K)$ of every physical resonance directly from the time signal. The k^{th} metabolite concentration is computed from the reconstructed amplitudes d_k as $C_{met} = d_k \times$ (25 μM/g ww).

Research for this project was evaluated in a formal application (June 2007, Dnr # 2007/709-31/1) to the Regional Ethics Committee at the Karolinska Institute. The Committee stated that they found no ethical issues that would preclude implementation of this research.

RESULTS

We present the Padé reconstructed positions and peak heights, and the computed concentrations for two partial signal lengths: N_P = 1000 and N_P = 1500, in the middle and right panels, respectively, of Table 1. At N_P = 1000 for each of the three cases: normal breast, fibroadenoma and breast cancer, only eight of the nine resonances were identified. In the interval where there should

have been two peaks, PCho (#4) at 3.2200 ppm and PE (#5) at 3.2202, only one resonance was identified at 3.2202 ppm. Prior to convergence at N_P = 1000, the peak height and concentration of PE were overestimated by approximately that of the missing PCho peak. Most of the other parameters and concentrations were fully correct at N_P = 1000, with the exception of the last digits within rounding error of the peak heights and/or concentrations of choline, glycerophosphocholine, β-glucose and taurine for the malignant case. At N_P = 1500, it is seen that full convergence was attained for all the reconstructed parameters for all nine resonances in each of the three cases. In earlier studies [23,24], we verified that the stability of convergence at higher signal length remained true at higher N_P including the full signal length N. In those studies [23,24] it was seen that of the 750 resonances, 741 were spurious Froissart doublets, since their amplitudes were zero such that the poles and zeros coincided. The remaining nine resonances were identified as genuine.

Padé-optimized magnetic resonance spectroscopy together with MR imaging might offer new possibilities for breast cancer screening, especially for high-risk groups

The absorption component shape spectra and the total shape spectra reconstructed by the FPT at two partial signal lengths N_P = 1000 and N_P = 1500 for the normal breast data are shown in Figure 1. These spectra are zoomed into the region between 3.2 ppm and 3.3 ppm. At N_P = 1000, as seen on the top right

PCho = phosphocholine
PE = phosphoethanolamine

Figure 1. Absorption component shape spectra [left panels (i) and (ii)] and total shape spectra [right panels (iii) and (iv)] as reconstructed by the fast Padé transform for normal breast from in vitro data of the study by Gribbestad et al. [25] within the interval of 3.2 ppm to 3.3 ppm. At partial signal length N_P = 1000 [top panels (i) and (iii)] the total shape spectrum is converged, but the component spectrum has not resolved PCho and has overestimated the height of phosphoethanolamine (PE). At partial signal length N_P = 1500 [bottom panels (ii) and (iv)] the two resonances PCho and PE are resolved with the correct heights, at 3.22 ppm. The small PCho peak completely underlies PE. Hereafter, the minus superscript in FPT$^{(-)}$ and P_K^-/Q_K^- denotes the variant of the FPT in terms of the inverse harmonic variable, $z^{-1} = e^{-i\tau\omega}$. The abscissae are in dimensionless units of ppm (parts per million) and the ordinates are in arbitrary units (au). Abbreviations for the metabolites are given in Table 1.

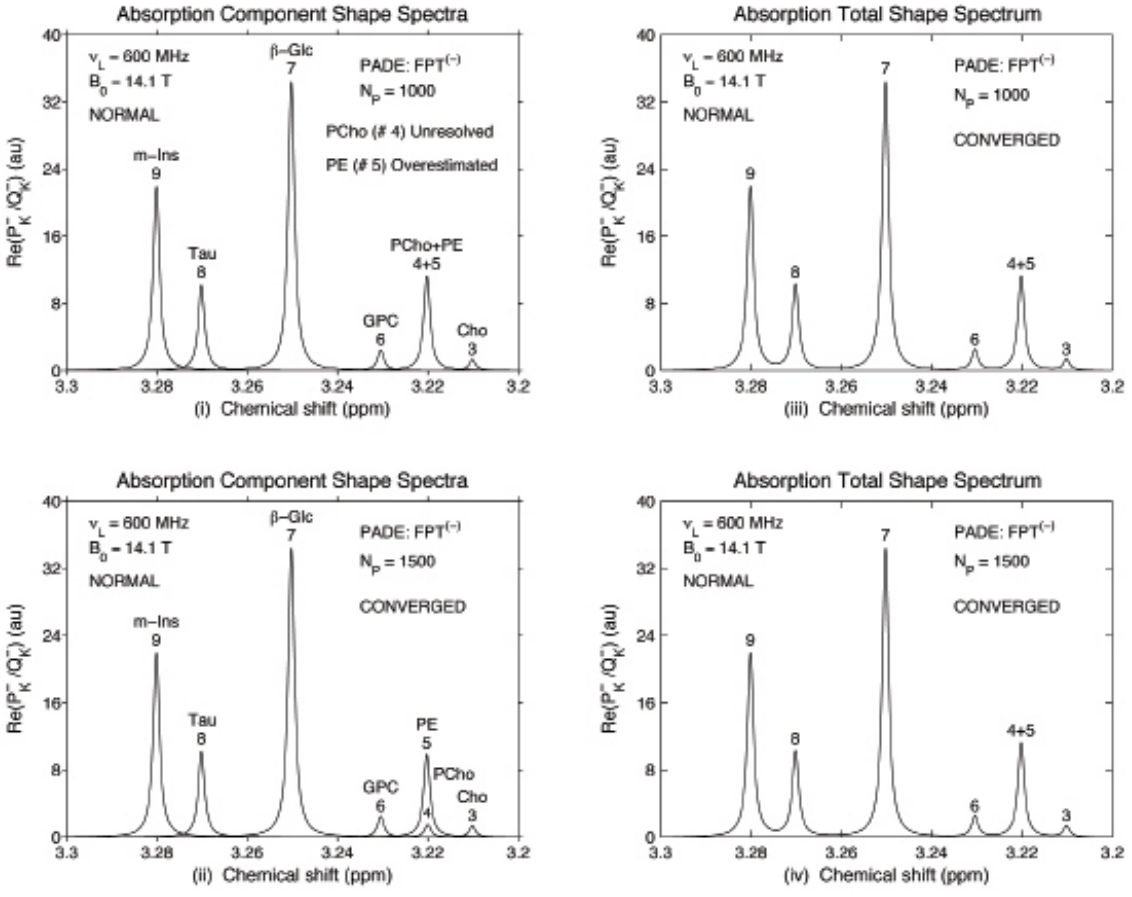

panel (iii), the absorption total shape spectrum is converged. However, this was not the case for the component shape spectrum [top left panel (i)], which shows a single peak (#5, PE) at 3.22, whereas peak #4 (PCho) remained unresolved. At N_P = 1500 in the bottom left panel (ii) of Figure 1, the component shape spectrum is converged, with both peaks ## 4 and 5 resolved and having the correct heights, as was the case for all the other peaks in the region between 3.2 ppm and 3.3 ppm. The small PCho peak completely underlies PE. In our earlier research [23,24] we confirmed the stability of convergence at longer partial signal lengths N_P for both the absorption component shape spectra and the total shape spectrum, and also for the full signal length N. Figures 2 and 3 show similar patterns for the fibroadenoma and breast cancer, with the relatively larger PCho still being undetected and PE overestimated on the component shape spectra at N_P = 1000, even though the absorption total shape spectrum converged at that signal length on panel (iii). The component shape spectra also converged for fibroadenoma and breast cancer at N_P = 1500. Convergence remained stable at longer partial signal lengths for both the absorption component shape spectra and the total shape spectrum, and at higher N_P including the full signal length N [23,24].

DISCUSSION

One of the key advantages of the fast Padé transform for analysis of MRS signals is its capability to resolve and precisely quantify closely overlapping resonances. This is most clearly illustrated in the spectrally dense region between 3.21 ppm and 3.23 ppm. It is most striking that phosphocholine and phosphoethanolamine are almost completely overlapping, separated by only about 0.0002 ppm, yet at convergence the FPT can still reconstruct the input parameters for these two resonances. Similarly, the FPT

Figure 2. Absorption component shape spectra [left panels (i) and (ii)] and total shape spectra [right panels (iii) and (iv)] as reconstructed by the fast Padé transform for fibroadenoma from in vitro data of Gribbestad's study [25] within the interval of 3.2 ppm to 3.3 ppm. At partial signal length N_P = 1000 [top panels (i) and (iii)] the total shape spectrum is converged, but the component spectrum has not resolved PCho and has overestimated the height of phosphoethanolamine (PE). At partial signal length N_P = 1500 [bottom panels (ii) and (iv)] the two resonances PCho and PE are resolved with the correct heights, at 3.22 ppm. The PCho peak completely underlies PE.

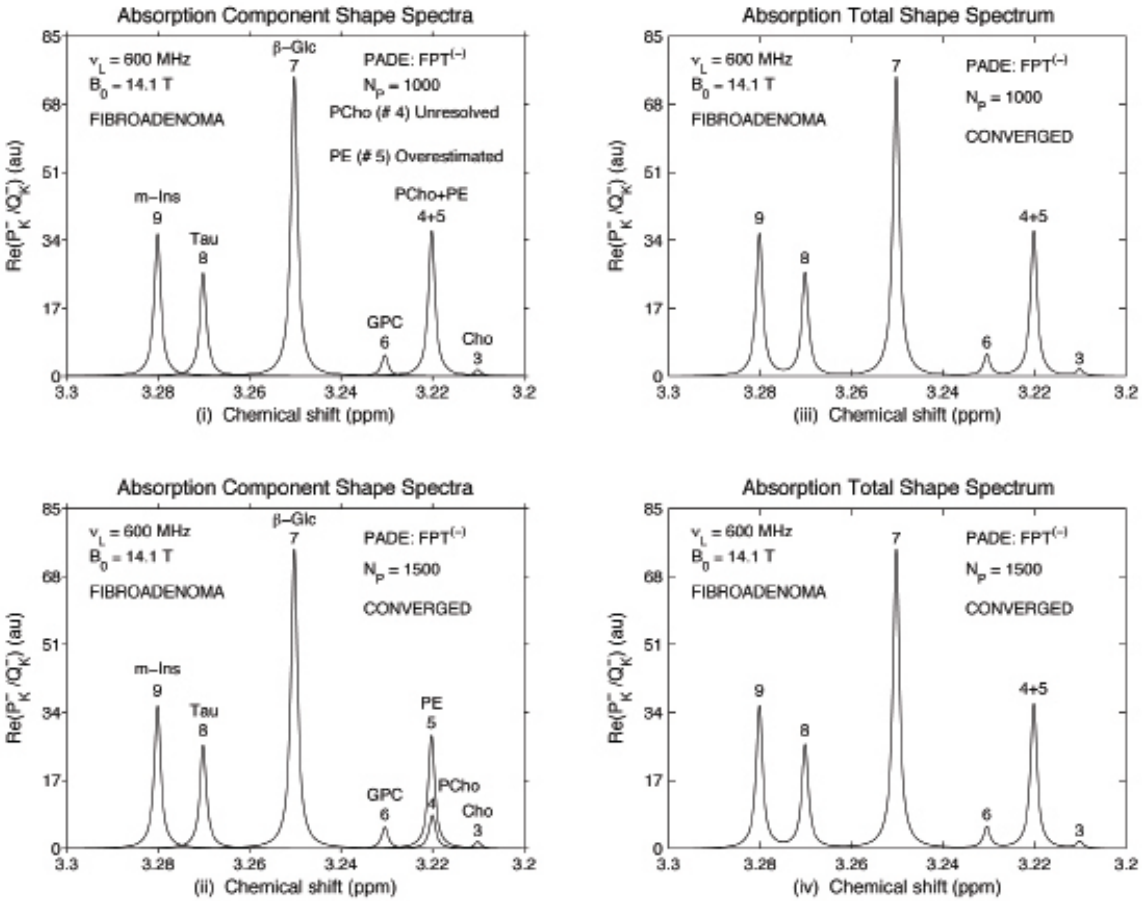

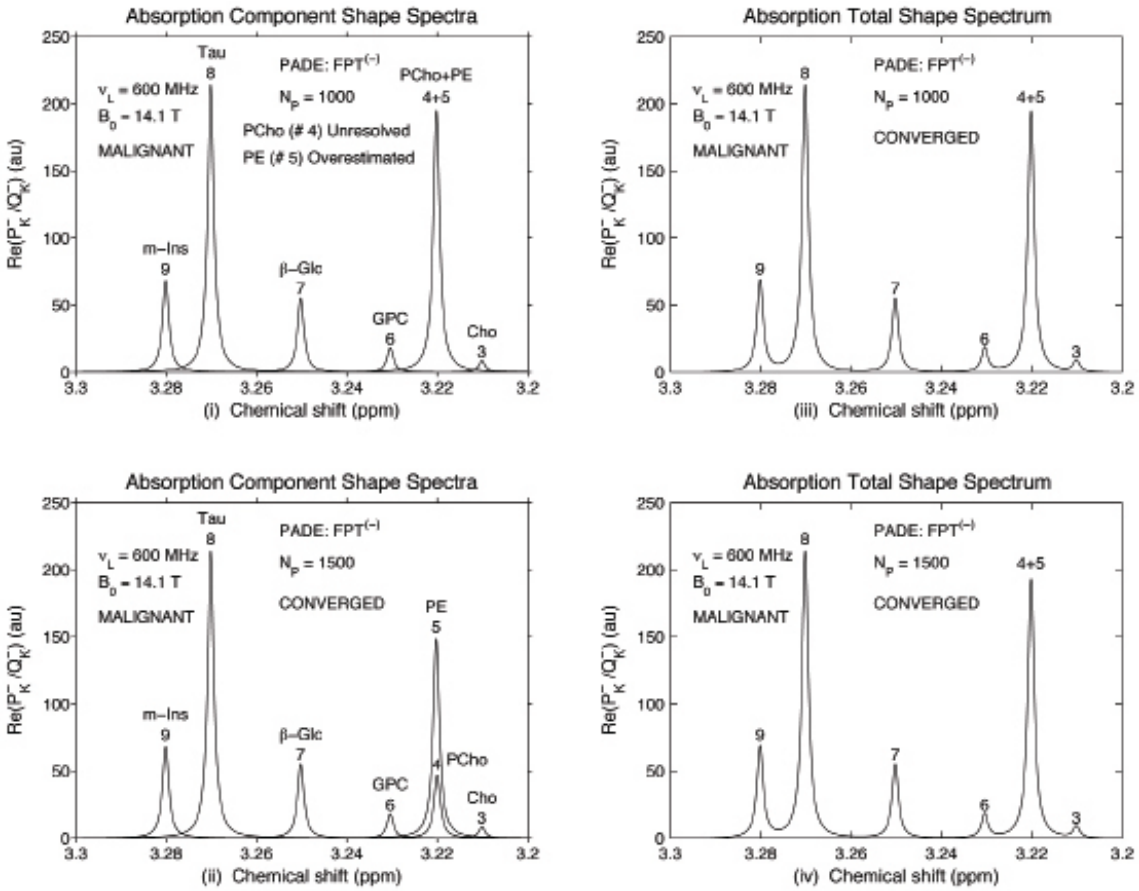

Figure 3. Absorption component shape spectra [left panels (i) and (ii)] and total shape spectra [right panels (iii) and (iv)] as reconstructed by the fast Padé transform for breast cancer from in vitro data of Gribbestad's study [25] within the interval of 3.2 ppm to 3.3 ppm. At partial signal length $N_P = 1000$ [top panels (i) and (iii)] the total shape spectrum is converged, but the component spectrum has not resolved PCho and has overestimated the height of phosphoethanolamine (PE). At partial signal length $N_P = 1500$ [bottom panels (ii) and (iv)] the two resonances PCho and PE are resolved with the correct heights, at 3.22 ppm. The PCho peak completely underlies PE.

has also been shown to exactly reconstruct all the resonances, including those that are extremely closely overlapping, from MRS time signals that closely matched time signals encoded via MRS from the brain of a healthy volunteer [28,29], as well as from normal and malignant prostate [23,30]. In all these cases, we observed that convergence of the total shape spectrum does not necessarily mean that this is the case for the component spectra. It is highly tenuous to attempt to surmise how many resonances underlie a given peak, as is done by post-processing fitting algorithms used in MRS [31-33]. Such an approach is the result of relying on Fourier-based processing, which can only generate a total shape spectrum. The fast Padé transform, on the other hand, not only extracts the spectral parameters exactly, but also unequivocally determines the number of resonances that are present [34]. This is vital for reliable quantification of all the metabolite concentrations [34].

It is clinically important for breast cancer diagnostics to identify and quantify the components of total choline. Our earlier analysis of the data from the study by Gribbestad et al. [25] reveals that the ratio of PCho/GPC is significantly higher in the malignant versus the normal breast tissue samples [35]. Data from human breast cell lines research reveal that a "glycerophosphocholine to phosphocholine switch" occurs with malignant transformation [36], associated with over-expression of the enzyme choline kinase responsible for PCho synthesis [37,38]. This reflects changes in membrane choline phospholipid metabolism. The main steps in choline metabolism proceed via the cytosine diphosphate-choline pathway [38]. Within that pathway, choline (3.21 ppm), PCho (3.22 ppm) and GPC (3.23 ppm) can be visualized in the proton magnetic resonance spectrum. Thus, it is necessary to analyze the relationship among these closely overlapping resonances. When these three metabolites are summed up as "total choline," as is conventionally done with in vivo MRS, salient information for breast cancer diagnostics

GPC = glycerophosphocholine

could well be missed. It should be noted, as well, that the distinction between fibroadenoma and breast cancer might also be facilitated, since the PCho concentration was about 5.7 times lower in the fibroadenoma than the median PCho concentration for breast cancer. This was percentually a greater difference than for PE or GPC. Here we can see that precise quantification of the components of total choline might be helpful for developing reliable databases to better distinguish benign and malignant breast pathology.

Since the input data for the present analyses come from a fairly small number of breast cancer samples and from only one fibroadenoma, no definitive conclusions can be made concerning which metabolites would best detect the presence of breast malignancy and distinguish this from normal tissue or benign lesions. Still, it is noteworthy that in our multiple logistic regression analysis [13] of the data from Gribbestad et al. [25], only lactate showed 100% diagnostic accuracy both with and without inclusion of the fibroadenoma. The diagnostic value of lactate is suggested by Sharma and co-authors [39] who used in vitro two-dimensional MRS to compare eleven involved and twelve uninvolved lymph nodes from patients with breast cancer. They found a highly significant difference between the lactate concentrations in involved and non-involved nodes. The increased lactate levels reflect the presence of cancer cells whose energy source is from the anaerobic glycolytic pathway. Further corroboration for the importance of assessing the rate of glycolysis and lactate clearance with respect to the diagnosis and prognosis of breast cancer is provided by animal models of breast cancer [40]. However, lactate has not yet been assessed as a metabolic marker of breast cancer in clinical in vivo MRS analyses.

The analyses in the present paper were based on noise-free time signals. This was done in order to show the fully controlled standard for the fast Padé transform. In a previous study [28] we explained why this approach is justified. Now we are extending our analysis to both noise-corrupted synthesized data (still well controlled) and to encoded time signals similar to those from Gribbestad's study [25] and with in vivo MRS data from the breast. These results will be reported soon.

We conclude that Padé-optimized MRS could certainly contribute to improving early breast cancer detection. Therefore, research along these lines should definitely continue with encoded data from benign and malignant breast tissue, in vitro and in vivo. It can be expected that Padé-optimized MRS will diminish the number of false positive findings using magnetic resonance-based modalities and will also enhance their sensitivity. Once this has been achieved, and considering that there is no exposure to ionizing radiation with magnetic resonance, new possibilities can emerge for screening and early detection. This could be especially pertinent for Israel, given the high risk of many women in the population. For example, Padé-optimized MRS could be used with greater surveillance frequency among younger women with high breast cancer risk.

Acknowledgments

This work was supported by Cancerfonden, the King Gustav the 5th Jubilee Fund, by the Signe and Olof Wallenius Stiftelse and the Karolinska Institute Research Fund, to which the authors are grateful.

Corresponding author:
Dr. K. (Edinger) Belkić
Dept. of Oncology-Pathology, Karolinska Institute, Building P-9, 2nd floor, Box 260, Stockholm SE-17176, Sweden
Phone: (46-8) 517-72494
email: Karen.Belkić@ki.se

References

1. Boyle P, Leon ME, Maisonneuve P, Autier P. Cancer control in women. Update 2003. *Int J Gynecol Obstet* 2003; 83 (Suppl 1): 179-202.
2. Hampel H, Sweet K, Westman JA, Offit K, Eng C. Referral for cancer genetics consultation: a review and compilation of risk assessment criteria. *J Med Genet* 2004; 4: 81-91.
3. www.nbcc.org.au 2006.
4. Saslow D, Boetes C, Burke W, et al. American Cancer Society guidelines for breast screening with MRI as an adjunct to mammography. *CA Cancer J Clin* 2007; 57: 75-89.
5. Fackenthal JD, Olopade OI. Breast cancer risk associated with BRCA1 and BRCA2 in diverse populations. *Nature Rev Cancer* 2007; 7: 937-48.
6. Calderon-Margalit R, Friedlander Y, Yanetz R, et al. Cancer risk after exposure to treatments for ovulation induction. *Am J Epidemiol* 2009; 169: 365-75.
7. Kloog I, Haim A, Stevens RG, Barchana M, Portnov BA. Light at night co-distributes with incident breast but not lung cancer in the female population of Israel. *Chronobiol Int* 2009; 26: 108-25.
8. Shaham J, Gurvich R, Goral A, Czerniak A. The risk of breast cancer in relation to health habits and occupational exposures. *Am J Ind Med* 2006; 49: 1021-30.
9. Shema L, Ore L, Ben-Shachar M, Haj M, Linn S. The association between breastfeeding and breast cancer occurrence among Israeli Jewish women: a case control study. *J Cancer Res Clin Oncol* 2007; 133: 539-46.
10. Keinan-Boker L, Vin-Raviv N, Liphshitz I, Linn S, Barchana M. Cancer incidence in Israeli Jewish survivors of World War II. *J Natl Cancer Inst* 2009; 101: 1489-500.
11. Allweis TM, Nissan A, Spira RM, Sklair-Levy M, Freund HR, Peretz T. Screening mammography for early diagnosis of breast cancer: facts, controversies, and the implementation in Israel. *Harefuah* 2003; 142: 281-6, 317 (Hebrew).
12. Cohen M, Azaiza F. Developing and testing an instrument for identifying culture-specific barriers to breast cancer screening in Israeli Arab women. *Acta Oncologica* 2008; 47: 1570-7.
13. Belkić K. Current dilemmas and future perspectives for breast cancer screening with a focus upon optimization of magnetic resonance spectroscopic imaging by advances in signal processing. *IMAJ Isr Med Assoc J* 2004; 6: 610-18.
14. Armstrong K, Moye E, Williams S, Berlin J, Reynolds E. Screening mammography in women 40 to 49 years of age: a systematic review for the American College of Physicians. *Ann Intern Med* 2007; 146: 516-26.
15. Kuni H, Schmitz-Feuerhake I, Dieckmann H. Mammography screening – neglected aspects of radiation risks. *Gesundheitswesen* 2003; 65: 443-6.
16. Schrading S, Kuhl CK. Mammographic, US, and MR imaging phenotypes of familial breast cancer. *Radiology* 2008; 246: 58-70.
17. Houssami N, Wilson R. Should women at high risk of breast cancer have screening magnetic resonance imaging (MRI)? *J Breast* 2007; 16: 2-4.
18. Iglesias A, Arias M, Santiago P, Rodríguez M, Mañas J, Saborido C. Benign breast lesions that simulate malignancy: magnetic resonance imaging with radiologic-pathologic correlation. *Curr Probl Diagn Radiol* 2007; 36: 66-82.
19. Essink-Bot ML, Rijnsburger AJ, van Dooren S, de Koning HJ, Seynaeve C. Women's acceptance of MRI in breast cancer surveillance because of a familial or genetic predisposition. *Breast* 2006; 15: 673-6.
20. Robson M. Breast cancer surveillance in women with hereditary risk due to BRCA1 or BRCA2 mutations. *Clin Breast Cancer* 2004; 5: 260-8.
21. Katz-Brull R, Lavin PT, Lenkinski RE. Clinical utility of proton magnetic resonance spectroscopy in characterizing breast lesions. *J Natl Cancer Inst* 2002; 94: 1197-203.
22. Tse GM, Yeung DK, King AD, Cheung HS, Yang WT. In vivo proton magnetic

resonance spectroscopy of breast lesions: an update. *Breast Cancer Res Treat* 2007; 104: 249-55.

23. Belkić Dž, Belkić K. Signal Processing in Magnetic Resonance Spectroscopy with Biomedical Applications. Boca Raton, FL: CRC Press Taylor & Francis Group, 2010.
24. Belkić Dž, Belkić K. Exact quantification of time signals from magnetic resonance spectroscopy by the fast Padé transform with applications to breast cancer diagnostics. *J Math Chem* 2009; 45: 790-818.
25. Gribbestad IS, Sitter B, Lundgren S, Krane J, Axelson D. Metabolite composition in breast tumors examined by proton nuclear magnetic resonance spectroscopy. *Anticancer Res* 1999; 19: 1737-46.
26. Belkić Dž. Exact analytical expressions for any Lorentzian spectrum in the fast Padé transform (FPT). *J Comp Meth Sci Engin* 2003; 3: 109-86.
27. Belkić Dž. Quantum Mechanical Signal Processing and Spectral Analysis. Bristol: Institute of Physics Publishing, 2005.
28. Belkić Dž. Exact quantification of time signals in Padé-based magnetic resonance spectroscopy. *Phys Med Biol* 2006; 51: 2633-70.
29. Belkić Dž. Machine accurate quantification in magnetic resonance spectroscopy. *Nucl Instrum Methods Phys Res* A 2007; 580: 1034-40.
30. Belkić Dž, Belkić K. Unequivocal resolution of multiplets in MR Spectra for prostate cancer diagnostics achieved by the fast Padé transform. *J Math Chem* 2009; 45: 819-58.
31. van der Veen JW, de Beer R, Luyten PR, et al. Accurate quantification of in vivo 31P NMR signals using the variable projection method and prior knowledge. *Magn Reson Med* 1988; 6: 92-8.
32. Vanhamme L, van den Boogaart A, van Haffel S. Improved method for accurate and efficient quantification of MRS data with use of prior knowledge. *J Magn Reson* 1997; 29: 35-43.
33. Provencher SW. Estimation of metabolite concentrations from localized in vivo proton NMR spectra. *Magn Reson Med* 1993; 30: 672-9.
34. Belkić Dž, Belkić K. Unequivocal disentangling genuine from spurious information in time signals: clinical relevance in cancer diagnostics through magnetic resonance spectroscopy. *J Math Chem* 2008; 44: 887-912.
35. Belkić Dž, Belkić K. Mathematical optimization of in vivo NMR chemistry through the fast Padé transform: Potential relevance for early breast cancer detection by magnetic resonance spectroscopy. *J Math Chem* 2006; 40: 85-103.
36. Aboagye EO, Bhujwalla ZM. Malignant transformation alters membrane choline phospholipid metabolism of human mammary epithelial cells. *Cancer Res* 1999; 59: 80-4.
37. Katz-Brull R, Seger D, Rivenson-Segal D, et al. Metabolic markers of breast cancer. Enhanced choline metabolism and reduced choline-ether-phospholipid synthesis. *Cancer Res* 2002; 62: 1966-70.
38. Glunde K, Jie C, Bhujwalla ZM. Molecular causes of the aberrant choline phospholipid metabolism in breast cancer. *Cancer Res* 2004; 64: 4270-6.
39. Sharma U, Mehta A, Seenu V, et al. Biochemical characterization of metastatic lymph nodes of breast cancer patients by in vitro 1H magnetic resonance spectroscopy: a pilot study. *Magn Reson Imaging* 2004; 22: 697-706.
40. Rivenzon-Segal D, Margalit R, Degani H. Glycolysis as a metabolic marker in orthotopic breast cancer, monitored by in vivo 13C MRS. *Am J Physiol Endocrinol Metab* 2002; 283: E623-30.